Comparing Generic and Vectorial Nonlinear Manoeuvring Models and parameter estimation using Optimal Truncated Least Square Support Vector Machine

Haitong Xu[a], Vahid Hassani[b,c], C. Guedes Soares[a*]

[a] Centre for Marine Technology and Ocean Engineering (CENTEC), Instituto Superior Técnico, Universidade de Lisboa, Av. Rovisco Pais, 1049-001 Lisboa, Portugal.
[b] Department of Mechanical, Electronics and Chemical Engineering, Oslo Metropolitan University, Oslo, Norway
[c] Department of Ships and Ocean Sstructures, SINTEF Ocean, Trondheim, Norway

*Corresponding author email: c.guedes.soares@centec.tecnico.ulisboa.pt;

ABSTRACT

An optimal truncated least square support vector machine (LS-SVM) is proposed for the parameter estimation of nonlinear manoeuvring models based on captive manoeuvring tests. Two classical nonlinear manoeuvring models, generic and vectorial models, are briefly introduced, and the prime system of SNAME is chosen as the normalization forms for the hydrodynamic coefficients. The optimal truncated LS-SVM is introduced. It is a robust method for parameter estimation by neglecting the small singular values, which contribute negligibly to the solutions and increase the parameter uncertainty. The parameter with a large uncertainty is sensitive to the noise in the data and have a poor generalization performance. The classical LS-SVM and optimal truncated LS-SVM are used to estimate the parameters, and the effectiveness of optimal truncated LS-SVM is validated. The parameter uncertainty for both nonlinear manoeuvring models is discussed. The generalization performance of the obtained numerical models is further tested against the validation set, which is completely left untouched in the training. The R^2 goodness-of-fit criterion is used to demonstrate the accuracy of the obtained models.

Keywords: Optimal truncated LS-SVM; System identification; Parameter uncertainty; Nonlinear manoeuvring model; Generalization performance.

NOMENCLATURE

m	Mass of the ship [kg]
I_{zz}	Yaw moment of inertia with Z-axis [kg m2]
x_G	Gravity centre of the ship in *x*-direction [m]
$\mu_{11}, \mu_{22}, \mu_{66}$	Added mass and moment [kg ; kg m]
X, Y, N	Dimensioned external forces and moment [N; N m]
$X_0', X_{uu}', X_{uuu}' \cdots$	Nondimensionalized hydrodynamic coefficients of surge motion
$Y_0', Y_{uv}', Y_{ur}', \cdots$	Nondimensionalized hydrodynamic coefficients of sway motion

$N_0', N_{uv}', N_{ur}', \cdots$	Nondimensionalized hydrodynamic coefficients of yaw motion
u,v,w	Velocity in surge, sway and heave [m/s]
p,q,r	The angular velocity of roll, pitch and yaw [rad/s]
$\dot{u}, \dot{v}, \dot{r}$	Acceleration of the surge, sway and yaw motions. [m/s^2; rad/s^2]
$\boldsymbol{\eta}$	Generalized position in *North-East-Down* frame [m]
$\boldsymbol{R}(\psi)$	Transfer matrix from Body frame to North-East-Down frame.
v	The velocity of a rigid body, expressed in Body-fixed frame
$\boldsymbol{M}_{RB}$	Rigid-body mass matrix
$\boldsymbol{M}_A$	Added mass matrix
$\boldsymbol{C}_{RB}(\boldsymbol{v})$	Rigid-body Coriolis-centripetal matrix
$\boldsymbol{C}_A(\boldsymbol{v})$	Added Coriolis-centripetal matrix
$D(\boldsymbol{v})$	Nonlinear damping matrix
$\boldsymbol{\tau}_{RB}$	Hydrodynamic forces and moments
S	Training set
w	Weight matrix
$\varphi(x)$	Mapping function
$K(x \cdot x)$	Kernel function
b	Bias term
C	Regularization factor
$L(\boldsymbol{w}, b, e_i, \alpha_i)$	Lagrange function
$\sum_{i=1}^{N} e_i^2$	Empirical error
A	Kernel matrix
Y	Output matrix
$\boldsymbol{\theta}$	Parameter matrix
U	Left-singular vectors
V	Right-singular vectors
Σ	Singular values matrix
U_r	Truncated left-singular vectors
V_r	Truncated right-singular vectors
Σ_r	Truncated singular values matrix
θ	Hydrodynamic coefficients matrix
y	Measurement data
V_y	Diagonal matrix of variances of y
$V_{\hat{\theta}}$	Error propagation matrix.
θ	Hydrodynamic coefficients matrix
$\sigma_{\hat{\theta}}$	Standard error of the parameters
R^2	The goodness of fit criterion

1. Introduction

Ship manoeuvrability is drawing more attention and is urgently required by the maritime industry, especially after International Maritime Organization (IMO) have added Autonomous Ships to its agenda in 2017. Autonomous shipping is in the future agenda of the maritime industry, however, safety and security are always the key factors need to be considered. The development of numerical computation makes it possible to simulate the ship response travelling with the complicated environmental disturbance. The vessel

simulators based on high-fidelity ship manoeuvring model plays an important role in the testing and verification of the complex system such as Dynamic positioning (DP) ships [1], ROVs operations and control systems [2,3], Ship Simulator [4,5], among others. It is also a good way to test the autonomous shipping system in the future.

Numerical models are widely used to describe the dynamic of marine ships. Many mathematical models have been proposed to meet different application considering the trade-off between the complexity and fidelity. For example, Abkowitz model, [6], is one of the most popular ones. The hydrodynamic forces and moments are approximated using 3-order truncated Taylor expansion techniques. This model has a good generalization performance, as well as its modified versions [7,8], but the disadvantage is that the model is complex and redundant, as many hydrodynamic coefficients have no physics meaning. The MMG model [9] approximates the forces on hull, propeller and rudder separately. Nomoto model [10] is a simplified linear model, is mostly used for autopilot design. The vectorial model proposed by Fossen (2011) is describing the motion of ships in a vectorial setting. Vectorial model benefits the designing controllers and observers for marine ships and the stability analysis. Sutulo and Guedes Soares proposed a model to describe arbitrary 3DOF ship manoeuvring motions [12,13].

Once the structure of the manoeuvring model is established, the next important tasks are to calculate the hydrodynamic coefficients. As described in the report by the Manoeuvring Committee of 24th International Towing Tank Conference [14], the hydrodynamic coefficients can be obtained using captive model tests, CFD calculations or system identification, just to name a few. Captive model test carried out in a multi-purpose towing tank, is a reliable and effective method to measure the hydrodynamic forces and moments, from which hydrodynamic coefficients in manoeuvring model can be identified [15]. System identification is a mature technique for building mathematical models of dynamical systems from measured data [16]. Now it has been widely used for estimation the hydrodynamics coefficients for marine vessels [8,17–23]. Least Square (LS) is one of the most widely used methods. Golding et al. [17][17] used the least square method to estimate the nonlinear viscous damping matrix of a marine surface vessel.   Ross *et. al* [22] estimated the hydrodynamic coefficients of a nonlinear manoeuvring model based on Planar Motion Mechanism (PMM) tests using the nonlinear least square method. The obtained manoeuvring model was then validated in full scale [24]. Sutulo and Guedes Soares [18], proposed an optimal offline system identification method

combining least squares with genetic algorithm to estimate the parameters of a nonlinear manoeuvring mathematical model.

However, there are some drawbacks of the least square methods, such as sensitivity to outliers and overfitting, and it usually leads to non-consistent estimations [25]. In order to get a robust estimation, truncated singular value decomposition (TSVD) [26] was used to solve the ill-conditioned problem of the least square method [27]. The least square method combined TSVD can get a robust estimation by neglecting the smaller singular values [28], because the data corresponding to smaller singular values usually imposes more uncertainty in the process of estimating uncertain parameters. Söderström, [29], used a regularized least-square method for parameter estimation of large data sets. Tikhonov regularization, [30], can also be used for solving the ill-posed problems. It can significantly improve the condition number by modifying the normal equations in the least square method while leaving the estimated parameter relatively unchanged. The effect of Tikhonov regularization is to estimate the parameters while also keep them near the reference values [31,32].

Many methods for system identification have been proposed for the modelling of marine vessels, such as, maximum likelihood method [21,33], Extended Kalman filter (EKF) [34,35], Support vector machine (SVM) [19]. SVM is a supervised machine learning algorithm that can be used for both classification [36] or regression [37]. Recently, SVM has been used to estimate the hydrodynamic coefficients for marine vessels. In [38], a least square support vector machine (LS-SVM) is used to identify a nonlinear steering model for ship autopilot design. Further results can be found in [39,40]. In [19], a least square support vector machine (LSSVM) was used to estimate the hydrodynamic coefficients of an Abkowitz model. The further work on this topic can be found in [41], in which, Particle Swarm Optimization was employed to choose the regularization factor. Hydrodynamic parameters of a catamaran were estimated using SVM by Luo *et. al* [20]. Hou and Zou, [42], identified a roll motion equation for floating structures in irregular waves was using a ε-support vector regression. In [43], used an optimal LS-SVM combined with artificial bee colony algorithm to estimate a dynamic model of a large container ship.

For parameter estimation, uncertainty analysis is always a challenging topic due to the noise. The parameter with a large uncertainty is not stable and the correspondent model usually has a poor generalization performance. As discussed in [7,41,44], the parameter drift happens when estimating the hydrodynamic

coefficients. The multicollinearity was considered the main reason for the parameter drift. Multicollinearity is commonplace in the regression analysis, mostly due to the redundancy of the structure of the model [13]. It is also called the ill-posed problem [27,28]. In [7], the dynamic cancellation was found and the linear hydrodynamic coefficients drift simultaneously using slender-body theory.

In [44], several methods, such as model simplification, parallel processing and additional excitation, were used to diminish the parameter drift. It needs to point out that the main purpose of these methods is to reconstruct the samples and lighten the multicollinearity. The parameters with large uncertainty easily drift from the true values. So, it is necessary to analyze the parameter uncertainty induced by the noise. In [45], the singular value decomposition was used to give an explanation of the parameter uncertainty. The least square methods combined with truncated singular value decomposition was used to diminish the parameter uncertainty and provide good results.

The main contribution of this paper is to propose an optimal truncated least square support vector machine (LS-SVM), and then use it to estimate the nondimensionalized coefficients of nonlinear manoeuvring models based on the captive model tests. A series of PMM tests, such as pure surge, pure drift, pure sway, pure yaw and mixed sway and yaw, was carried out by SINTEF Ocean in their multi-purpose towing tank using a scaled ship model of research vessel Gunnerus [24]. The optimal truncated LS-SVM is different from the method in the references [46,47], where singular value decomposition (SVD) was employed for signal pre-processing, and the filtered data was then used for training the classical LS-SVM. The proposed method is trained by the singular value decomposition (SVD) of the kernel matrix. So, it can avoid the costly matrix inversion operation in classical LS-SVM. Meanwhile, the robust estimation can be achieved by ignoring the smaller singular values, because of their negligible contribution to the solutions. The optimal constant is estimated using *L-curve*, which plays the trade-off between the size of a regularized solution and its fit to the given data. In order to demonstrate the performance of the optimal truncated LS-SVM, classical LS-SVM was firstly used to estimate the parameters and then the validation process was carried out based on the obtained numerical model. The second contribution is to compare the performance of the generic and vectorial nonlinear manoeuvring models. The parameter uncertainty for both nonlinear manoeuvring models is discussed, and the generalization performance of the resulted numerical models was further tested against the validation set, which was completely left untouched in the training.

5

The rest paper is organized as follows. Section 2 describes both generic and vectorial nonlinear manoeuvring models for the marine surface vessel. In section 3, the classical LS-SVM and optimal truncated LS-SVM are introduced. Planar motion mechanism (PMM) Tests is briefly described in Section 4. In section 5, the parameter estimates for the generic and vectorial model is carried out using the optimal truncated LS-SVM. The parameter uncertainty is also discussed in this section. The final section is the conclusion.

2. Nonlinear Manoeuvring models for marine surface vessel

2.1 Generic Nonlinear Manoeuvring Model

Usually, the motions of a marine surface can be described in 6 Degree of Freedoms (DOFs), as illustrated in Fig.1. They are surge, sway, heave, roll, pitch and yaw. The manoeuvring motion of a traditional merchant ship typically occurs with a much lower frequency than the wave encounter frequencies [48]. So, it is reasonable to neglect the fluid-memory effects [11]. The coordinate frames of a surface ship moving in a horizontal plane are presented in Fig.2. In order to describe the dynamics of the ship, a manoeuvring mathematical model need to be derived. Without loss of generality, any marine ships can be treated as the free rigid body moving under the action of the external forces and moments. The Euler equations of arbitrary motion in the horizontal plane are given:

$$\left(m+\mu_{11}\right)\dot{u}-mvr-mx_{G}r^{2}=X$$
$$\left(m+\mu_{22}\right)\dot{v}+\left(mx_{G}+\mu_{26}\right)\dot{r}+mur=Y \qquad (1)$$
$$\left(mx_{G}+\mu_{26}\right)\dot{v}+\left(I_{zz}+\mu_{66}\right)\dot{r}+mx_{G}ur=N$$

where, m and I_{zz} are the mass and the moment of inertia, respectively. x_{G} is the centre-of-mass' coordinates. μ_{11}, μ_{22} and μ_{26} are the add-masses and moments, respectively. X, Y and N are the hydrodynamic forces and moments.
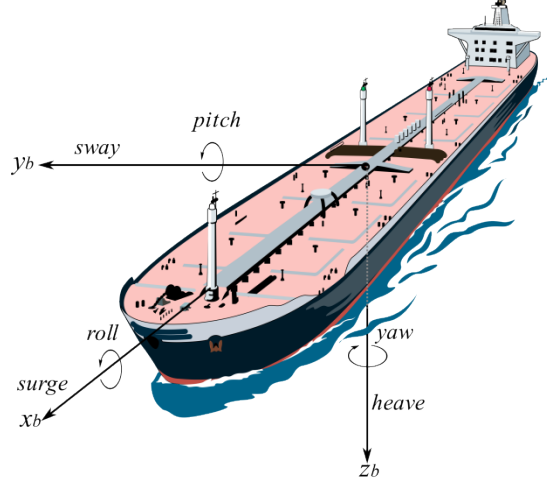
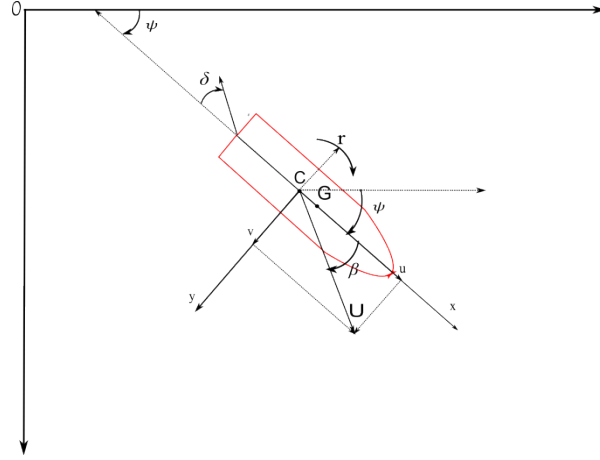Fig. 1. Marin surface ships motions in 6 DOFs

Figure 2: Coordinate frames for marine surface vehicle

In order to simplify the problem, it is assumed that the origin of the central body axes is at the centre of mass. The quasi-polynomials regression models for the surge, sway forces and yaw moment expressed in the nondimensionalized forms [49] are here taken in the forms [15]:

$$X'(v',r') = -\mu'_{11}\dot{u}' + X'_0 + X'_{vv}v'v' + X'_{vr}v'r' + X'_{rr}r'r' \tag{2}$$

$$Y'(v',r') = -\mu'_{22}\dot{v}' - \mu'_{26}\dot{r}' + Y'_0 + Y'_v v' + Y'_r r' + Y'_{v|v|}v'|v'| + Y'_{v|r|}v'|r'| \tag{3}$$

$$N'(v',r') = -\mu'_{26}\dot{v}' - \mu'_{66}\dot{r}' + N'_0 + N'_v v' + N'_r r' + Y'_{r|v|}r'|v'| + N'_{v|r|}v'|r'| + N'_{r|r|}r|r| \tag{4}$$

7

Here, the forces and moments due to the water around the ship are also included in the equations. As presented in [13], the quasi-polynomials regression models can be slightly more economical considering the number of terms and computation speed.

In order to compare the coefficients of different ships and to estimate the dynamics of a full-size ship, the hydrodynamic parameters need to be converted to dimensionless ones. The prime system recommended by SNAME [49] will be used to normalize the hydrodynamic coefficients. The water density, ρ, the ship length L and the ship speed U are employed as the characteristic dimensional parameter. The forces are normalized with $0.5\rho L^2 U^2$ and the moment with $0.5\rho L^3 U^2$. The nondimensionalized velocities and yaw rate are: $u' = u/U, v' = v/U, r' = rL/U$. The list of the nondimensionalization factors and corresponding coefficients in Eqs. (2-4) is shown in Table 1.

Table 1. Dimensional factors for nondimensionalized the hydrodynamic coefficients.

Coef.	Dimensional Factor	Coef.	Dimensional Factor	Coef.	Dimensional Factor
μ'_{11}	$0.5\rho L^3$	μ'_{22}	$0.5\rho L^3$	μ'_{26}	$0.5\rho L^4$
X'_0	$0.5\rho L^2 U^2$	μ'_{26}	$0.5\rho L^4$	μ'_{66}	$0.5\rho L^5$
X'_{vv}	$0.5\rho L^2$	Y'_0	$0.5\rho L^2 U^2$	N'_0	$0.5\rho L^3 U^2$
X'_{vr}	$0.5\rho L^3$	Y'_v	$0.5\rho L^2 U$	N'_v	$0.5\rho L^3 U$
X'_{rr}	$0.5\rho L^4$	Y'_r	$0.5\rho L^3 U$	N'_r	$0.5\rho L^4 U$
		$Y'_{v|v|}$	$0.5\rho L^2$	$N'_{r|v|}$	$0.5\rho L^4$
		$Y'_{v|r|}$	$0.5\rho L^3$	$N'_{v|r|}$	$0.5\rho L^4$
				$N'_{r|r|}$	$0.5\rho L^5$

2.2 Vectorial Nonlinear Manoeuvring Model

Vectorial nonlinear manoeuvring model is widely for marine control design and stability analysis. It was proposed in Fosen [11], and now received attention of others [43,50,51]. The manoeuvring model is written in a vectorial setting with emphasis placed on matrix properties like positiveness, symmetry and skew-symmetry [52]. Those properties benefit the marine control system design (controller and observer) [11]. A nonlinear manoeuvring model in vectorial setting for a marine surface vessel in 3-DOF (surge, sway and yaw) can be expressed as [11,53]:

$$\dot{\eta} = R(\psi)v$$

$$M_{RB}\dot{v} + C_{RB}(v)v + M_A\dot{v} + C_A(v)v + D(v)v = \tau_{prop} + \tau_{rudder} + \tau_{wind} + \tau_{wave} + \tau_{ext.} \tag{5}$$

where, $\eta = [N, E, \psi]^T$ are the generalized position defined in the *North-East-Down* (NED). $v = [u, v, r]^T$ is

the velocity and yaw rate in the body-fixed frame. M and M_A are the mass matrix and added mass matrix.

$C_{RB}(v)$ and $C_A(v)$ are the Coriolis-centripetal matrix of the rigid-body and hydrodynamic Coriolis-

centripetal matrix, respectively. $D(v)$ is the hydrodynamic damping matrix. $R(\psi)$ is the rotation matrix

achieving the transformation of linear velocity from BODY to NED.

$$R(\psi) = \begin{bmatrix} \cos(\psi) & -\sin(\psi) & 0 \\ \sin(\psi) & \cos(\psi) & 0 \\ 0 & 0 & 1 \end{bmatrix} \tag{6}$$

The mass matrix and Coriolis-centripetal matrix of the rigid-body, $C_{RB}(v)$, is given:

$$M_{RB} = \begin{bmatrix} m & 0 & 0 \\ 0 & m & 0 \\ 0 & 0 & I_z \end{bmatrix} \tag{7}$$

$$C_{RB} = \begin{bmatrix} 0 & 0 & -mv \\ 0 & 0 & mu \\ mv & -mu & 0 \end{bmatrix} \tag{8}$$

Added-mass matrix and hydrodynamic Coriolis-centripetal matrix, $C_A(v)$, is given as in [11]:

$$M_A = \begin{bmatrix} X_{\dot{u}} & 0 & 0 \\ 0 & Y_{\dot{v}} & Y_{\dot{r}} \\ 0 & N_{\dot{v}} & N_{\dot{r}} \end{bmatrix} \tag{9}$$

$$C_A(v) = \begin{bmatrix} 0 & 0 & Y_{\dot{v}}v + Y_{\dot{r}}r \\ 0 & 0 & -X_{\dot{u}}u \\ -Y_{\dot{v}}v - Y_{\dot{r}}r & X_{\dot{u}}u & 0 \end{bmatrix} \tag{10}$$

The nonlinear damping matrix is given:

$$D(\mathbf{v}) = \begin{bmatrix} -X_{uuu}u^2 - X_{uvr}vr & -X_{uvv}uv & -X_{urr}ur \\ 0 & -Y_{uuv}u^2 - Y_{|v|v}|v| & -Y_{uur}u^2 - Y_{|v|r}|v| \\ 0 & -N_{uuv}u^2 - N_{|r|v}|r| & -N_{uur}u^2 - N_{|v|r}|v| - N_{|r|r}|r| \end{bmatrix} \quad (11)$$

Here, The viscous damping matrix is usually over-modelled, as presented in [45,54]. This viscous damping matrix is trying to combine the similar terms of two types, quasi-polynomials and cubic-polynomial, such as $r|r|$ and r^3, as commented in [13]. This operation will results in overfitting as presented in our previous paper. The nonlinear damping matrix in Eq. (11) can usefully reproduce the PMM test and diminished the overfitting. During the captive model tests, the measured forces in the 3DOF nonlinear manoeuvring model described in Eq. (5) can be written as:

$$\tau_{RB} = M_A \dot{\mathbf{v}} + C_A(\mathbf{v})\mathbf{v} + D(\mathbf{v})\mathbf{v} \quad (12)$$

The equations of the hydrodynamic forces and moment can be expressed as follow:

$$X' = X'_{\dot{u}}\dot{u} + Y'_{\dot{v}}vr + Y'_{\dot{r}}rr + X'_{uuu}uuu + X'_{uvv}uvv + X'_{rvu}rvu + X'_{urr}urr \quad (13)$$

$$Y' = X'_{\dot{u}}ur + Y'_{\dot{v}}\dot{v} + Y'_{uuv}uuv + Y'_{v|v|}v|v| + Y'_{\dot{r}}\dot{r} + Y'_{uur}uur + Y'_{r|v|}r|v| \quad (14)$$

$$N' = Y'_{\dot{r}}ur + (Y'_{\dot{v}} - X'_{\dot{u}})vu + N'_{\dot{r}}\dot{r} + N'_{uur}uur + N'_{r|r|}r|r| + N'_{\dot{v}}\dot{v} + N'_{uuv}uuv + N'_{v|r|}v|r| + N'_{r|v|}r|v| \quad (15)$$

As presented in Eq.(15), the term $(Y'_{\dot{v}} - X'_{\dot{u}})vu$ is the Munk moment, which causes a destabilizing moment on a ship with steady oblique translator motion [48]. It arises for a simple reason, the asymmetric location of the stagnation points where the pressure is highest on the front of the body and lowest on the back. It tends to rotate the ship perpendicular to the flow. That is the principal reason for the necessity of stabilizing fins on submarine and torpedo hulls.

3. Optimal Truncated least square support vector machine and parameter uncertainty analysis

Support Vector Machine (SVM) is a classical machine learning algorithm. It was proposed by Vapnik (1995). It can also be considered a special case of Tikhonov regularization [30]. It solves the optimization problem by searching the maximum-margin hyperplane, which separates the data points. So, it was used for classification at the beginning and then extended for regression purpose [55,56]. Least square support vector machine (*LS-SVM*) is a modified version of SVM proposed by Suykens and Vandewalle (1999). By including the regularized square error term in the SVM, the solutions can be obtained by solving a set of linear equations instead of a convex quadratic programming (QP) problem for classical SVMs. However, the LS-SVM lost the sparseness feature [57].

In this section, the standard LS-SVM will be introduced briefly. Then a modified version, truncated LS-SVM, is proposed by including singular value decomposition technology. Truncated LS-SVM is training through the singular value decomposition (SVD) of the kernel matrix. So, it can avoid the matrix inversion operation, which is usually computationally expensive. Meanwhile, the truncated LS-SVM also neglect the effect of the small singular values and can provide a robust estimation.

3.1 Classical Least square support vector machine

Given the training set, which contains N pairs of data, $\boldsymbol{S} = \{s_i \mid s_i = (x_i, y_i), x_i \in \mathfrak{R}^n, y_i \in \mathfrak{R}\}_{i=1}^N$, where x_i is the input and y_i is the output. As presented in [55], the general approximation function of SVM is given:

$$y(x) = \boldsymbol{w}^T \boldsymbol{\varphi}(x) + b \qquad (16)$$

where x is the training samples; $y(x)$ are the target values; b is the bias term; $\boldsymbol{w}$ is a weight matrix; $\boldsymbol{\varphi}(x)$ is mapping function that map the training data, x_i, to a higher dimensional feature space [55]. For function estimation or regression purpose, the following optimization problem is formulated:

$$\min_{w,b,e_i} \quad J(w,e) = \frac{1}{2}\boldsymbol{w}^T \boldsymbol{w} + \frac{1}{2}C\sum_{i=1}^{N} e_i^2 \qquad (17)$$

11

subject to the equality constraints:

$$s.t. \qquad y_i = w^T \varphi(x_i) + b + e_i, \quad i = 1, \cdots, N \qquad (18)$$

where $e_i, i = 1 \cdots N$, is the error, and C is the regularization factor. It balances the model accuracy and the model complexity, which also known as structural risk [55]. In order to solve this optimization problem, the Lagrange function needs to be constructed and given as:

$$L(w, b, e_i, \alpha_i) = \frac{1}{2} w^T w + \frac{1}{2} C \sum_{i=1}^{N} e_i^2 - \sum_{i=1}^{N} \alpha_i [w^T \varphi(x_i) + b + e_i - y_i] \qquad (19)$$

where α_i are the Lagrange multipliers. The optimality condition, Karush-Kuhn-Tucker conditions (KKT) [55], are given by:

$$
\begin{aligned}
\frac{\partial L}{\partial w} &= 0 \quad \rightarrow \quad w = \sum_{i=1}^{N} \alpha_i \varphi(x_i) \\
\frac{\partial L}{\partial b} &= 0 \quad \rightarrow \quad \sum_{i=1}^{N} \alpha_i = 0 \\
\frac{\partial L}{\partial e_i} &= 0 \quad \rightarrow \quad \alpha_i = C e_i \quad i = 1, \cdots, N \\
\frac{\partial L}{\partial \alpha_i} &= 0 \quad \rightarrow \quad w^T \varphi(x_i) + b + e_i - y_i = 0 \quad i = 1, \cdots, N
\end{aligned}
\qquad (20)
$$

Eliminate the variable w and e_i, one gets the following solution:

$$\underbrace{\begin{bmatrix} 0 & \vec{1} \\ \vec{1} & K(\cdot) + C^{-1} I \end{bmatrix}}_{A} \underbrace{\begin{bmatrix} b \\ \vec{\alpha} \end{bmatrix}}_{\theta} = \underbrace{\begin{bmatrix} 0 \\ \vec{Y} \end{bmatrix}}_{Y} \qquad (21)$$

where I is an $N \times N$ identity matrix. $\vec{\alpha} = [\alpha_1, \cdots \alpha_N]^T$, $\vec{Y} = [y_1, \cdots, y_N]^T$. $K(x_k \cdot x_i) = \varphi(x_k)^T \varphi(x_i)$, $i = 1, \cdots, N$ is the kernel function, which represents an inner product between its operands. It is positive

definite and satisfies the Mercer condition [36,37]. In this paper, for parameter estimation, the linear kernel function is chosen. So, the resulting LS-SVM model for the regression is given:

$$y(x) = \sum_{i=1}^{N} \alpha_i K(x \cdot x_i) + b \qquad (22)$$

As presented in Eq. (21), the dimension of the matrix, A, is $(N+1) \times (N+1)$. It is proportion to the length of the training set. So, if there is large data in the training set, the classical LS-SVM fails to inverse the matrix due to the heavy computation. In the following phase, an optimal truncated LS-SVM is proposed to solve the parameter estimation for a large-scale problem.

3.2 Optimal Truncated LS-SVM and uncertainty analysis

As described in [7,44], the hydrodynamic coefficients usually drift from the true values using the system identification method. The obtained parameters are usually dominated by the noise, and with a large uncertainty. In [7,44], the multicollinearity happens during the parameter estimation, and several methods, such as additional excitation, parallel processing, exaggerated over-and underestimation et. al, were used to diminish the parameter uncertainty. The main purpose of these methods is to reconstruct the sample and lighten the multicollinearity of variables. In this phase, parameter uncertainty is discussed using singular value decomposition. Then, a truncated least square support vector machine is proposed to diminish the parameter drift. Firstly, using the singular value decomposition, the kernel matrix, A, can be rewritten as:

$$A = \sum_{i=1}^{n} u_i \sigma_i v_i^T = U \Sigma V^T \qquad (23)$$

Then, the Eq. (21) can be rewritten as:

$$\theta = \left(U \Sigma V^T \right)^{-1} Y = V \Sigma^{-1} U^T Y = \sum_{i=1}^{n} \frac{v_i u_i^T}{\sigma_i} Y \qquad (24)$$

where the matrix U and V are orthonormal, $U^T U = I$ and $V^T V = I$. $\square$ is the diagonal matrix of the singular values of the matrix X. Assume that there is an additive perturbation, δY, it will propagate to a perturbation in the solution,

$$\delta \theta = V \Sigma^{-1} U^T \delta y = \sum_{i=1}^{n} \frac{v_i u_i^T}{\sigma_i} \delta Y \qquad (25)$$

13

As presented in Eq. (25), when the singular value, σ_i, is very small or close to the numerical precision of the computation, then the perturbation in the y is magnified and potentially dominate the solutions, θ_i. The corresponding columns of U and V contribute negligibly to the matrix A. Their contribution to the solution can be easily dominated by the noise and round-off error in y. So, the obtained parameters are dominated by the noise. As discussed in the preceding section, the number of the singular, σ_i, equals to the length of the training data. The obtained parameters are inevitably dominated by the smaller singulars and are easily affected by the noise in the data and drift from the true values with a large probability. In order to diminish such uncertainty and obtain a robust estimation, it is necessary to neglect the effect caused by the smaller singular values. Truncated singular value decomposition (TSVD) can be used to obtain a relatively accurate representation of the matrix, A, by retaining the first r singular values of A and the corresponding columns of U and V. The TSVD can be presented as

$$A_r = U_r \Sigma_r V_r^T \qquad\qquad (26)$$

where the matrix Σ_r is obtained by retaining the first r singular values of Σ. Similarly, matrices U_r and V_r are found using the corresponding singular vectors. The resulting A_r represents the reduced data set where the data related to the omitted singular values are filtered. The optimal value of r can be estimated using the *L-curve* [31]. It is a log-log plot of the norm of a regularized solution versus the norm of the corresponding residual norm. it is a graphical tool for displaying the trade-off between the size of a regularized solution and its fit to the given data, as the r varies [30,58]. From the L-curve plot, it is convenient to get the optimal parameters. The whole program is give in Fig. 3.
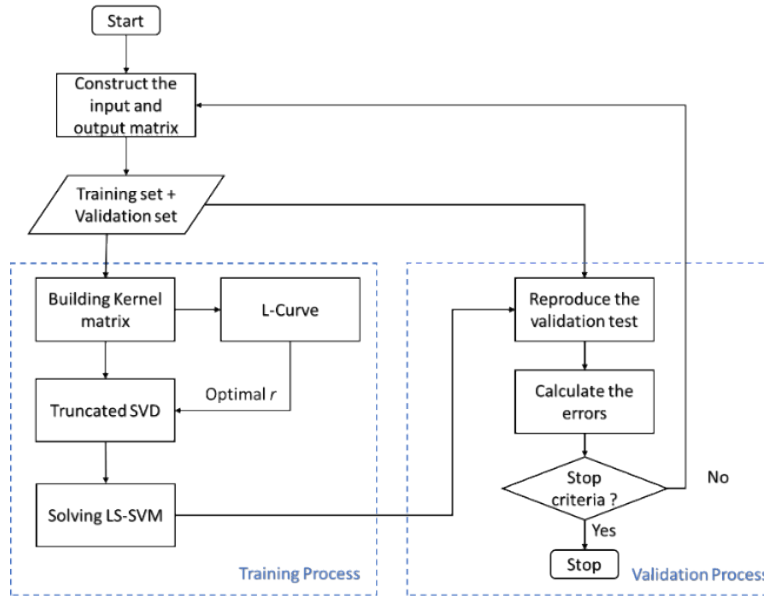
Fig. 3. Flowchart of Optimal Truncated LS-SVM

4. Planar Motion Mechanism (PMM) Tests

This section summarizes the series of captive model tests carried out by SINTEF Ocean during a research project [59] on the scaled ship model according to the recommended procedures by ITTC [60]. The main particulars of the research vessel are given in Table 1. Captive model test are nowadays commonly used for modelling the ship motions. They can provide a rich information for system identification method and get a reasonable estimation of the hydrodynamic coefficients, however, performing such tests is costly. Here, a brief summary of different PMM tests is presented, such as pure surge, pure drift, pure sway, pure yaw and mixed sway and yaw, which were carried out in SINTEF Ocean's multi-purpose towing tank using the scaled ship model, presented in Fig. 4. The motions in the surge, sway and yaw were controlled using a 6-DOF hexapod motion platform, which is mounted on the carriage.

Pure surge test tows the model forward with oscillations around a fixed velocity. It is usually sinusoidal oscillations. During the tests, the sway speed and yaw rate are kept as zero ($v=0$ and $r=0$). So, the effect of sway and yaw can be eliminated from the surge motion model. This test aims to achieve the full response of surge motion. The pathline of pure surge is presented in the Fig. 5(a).

15

Table 1. Main particulars of the Marine Research Vessel

Item	Description
Length over all (Loa)	31.25 m
Length between pp (Lpp)	28.9 m
Length in waterline (Lwl)	29.90
Draught (D)	2.75 m
Beam (B)	9.6 m
Block coefficient (Cb)	0.569
Deadweight	107 t
Displacement (Δ)	45 t
Volume Displacement (∇)	436.672 m3
Bow tunnel thruster	1
Number of Rudder	2
Speed at 100% MCR	12,6 kn
Cruising speed	9,4 kn
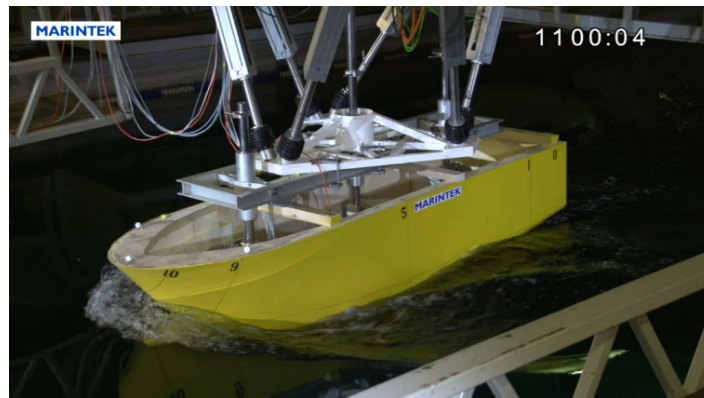
Fig. 4. Planar motion mechanism tests (PMM) in a towing tank [courtesy of SINTEF OCEAN]
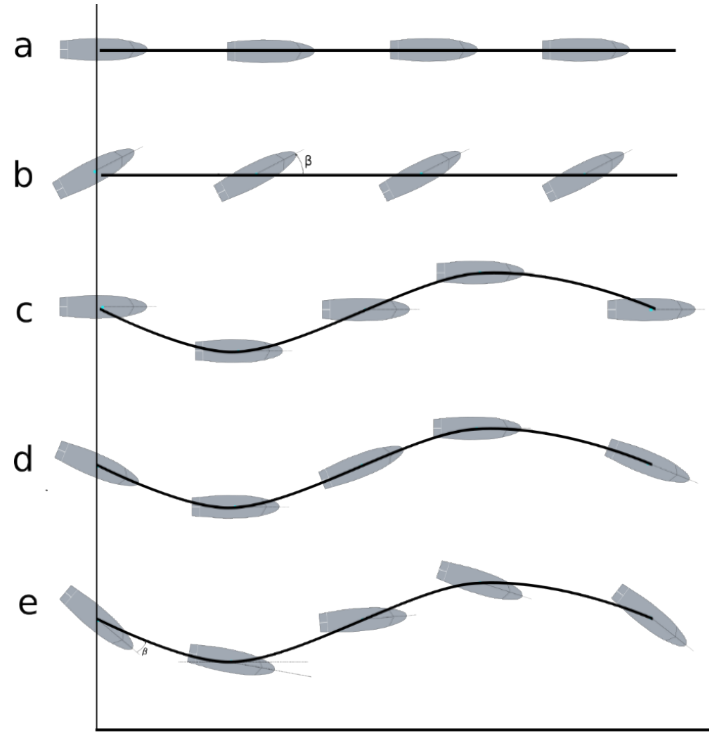
Fig. 5. PMM test of ship model travelling along the pathline: (a) straight line (pure suge or surge acceleration); (b) pure drift; (c) pure sway; (d) pure yaw; (e) pure yaw +drift

Pure drift test tows the mode forward with a fixed drift angle β, as presented in Fig. 5(b). During the test, the surge and sway velocity is a non-zero constant, while the yaw rate is zero ($u = U\cos(\beta), v = U\sin(\beta), r = 0$, $v = v_{max}\cos(\omega t)$). So, the hydrodynamic coefficients related to the yaw motion can be neglected.

Pure sway test is used to isolate the sway dynamics from the yaw motion. The ship will move forward with a constant velocity and with a sinusoidal oscillation in Sway, where $u = u_c$, $v = v_{max}\cos(\omega t)$ and $\psi = 0$, as presented in Fig. 5(c). The hydrodynamic coefficients related to the yaw motion can be neglected during the identification process. This test aims to achieve the full response of sway motion.

Pure yaw test is used to isolate the sway dynamics from the yaw motion. During the test, the ship moves forward with a constant velocity and with a sinusoidal oscillation in sway motion where $u = u_c$, $v = 0$ and $\psi = \psi_{max}\sin(\omega t)$, as presented in Fig. 5(d). This test aims to achieve the full response of sway motion.

Pure Sway and drift were carried out using a ship model with a sinusoidal oscillation in sway motion and a constant drift angle. The pathline is presented in the Fig. 5(e). This test can provide the dynamic information of surge, sway and yaw motion. So, it can be used to estimate the coefficients related to the surge, sway and yaw motion. During the test, the ground speed and drift angle is kept as constant, and yaw rate are set as a sinusoidal oscillation, $U = U_c$, $\beta = \beta_c$ and $\psi = \psi_{max} \sin(\omega t)$

5. Estimate the Nonlinear Hydrodynamic coefficients and validation

In this section, the parameter estimation for the nonlinear manoeuvring model is presented. Firstly, as illustrated in Fig. 3, whole PMM test data are divided into the training set and validation set. The training set is used to train the LS-SVM model and identify the hydrodynamic coefficients. The validation or test set is completely left untouched within the training process and is used to check the performance of the trained model on fresh data. With the training set, the classical LS-SVM is firstly employed to estimate the hydrodynamic coefficients. The uncertainty of obtained parameters is also provided. Then, the proposed method, optimal truncated LS-SVM, is used to estimate the hydrodynamic coefficients. The obtained numerical model is going to reproduce the validation set.

Before the identification process, the above equations (2) to (4) need to be reordered in a vector format given by:

$$X\theta = y \qquad\qquad (27)$$

where the matrix X contains the measured data. In this study, a small portion data is used for the training set, for surge and sway motions, the 7000 pairs of data are chosen as the training set, and 6000 pairs of data for yaw motion. It includes the pure drift, harmonic sway, harmonic yaw and mixed yaw and drift. The whole tests, (around 70000 pairs), are chosen as the validation set. The test set includes the training set and the fresh data, which is completely left untouched within the training process. θ represents the uncertain parameters described in equation (28), and y is the matrix of the recorded forces and moments during the tests. Obviously, the linear equation is over-determined, because the length of the training data, (n), is bigger than the number of the parameters ($n>m$). The vectors of parameters are given:

18

$$\theta_{surge} = \begin{bmatrix} \dot{u}', X'_0, X'_{vv}, X'_{vr}, X'_{rr} \end{bmatrix}$$
$$\theta_{sway} = \begin{bmatrix} \mu'_{22}, \mu'_{26}, Y'_0, Y'_v, Y'_r, Y'_{v|v|}, Y'_{v|r|} \end{bmatrix} \qquad\qquad (28)$$
$$\theta_{yaw} = \begin{bmatrix} \mu'_{26}, \mu'_{66}, N'_0, N'_v, N'_r, Y'_{r|v|}, N'_{v|r|}, N'_{r|r|} \end{bmatrix}$$

The condition number is usually used to indicate how sensitive a function is to changes or errors in the input, and how much error in the output results from an error in the input. So, If the condition number is large, then it is ill-conditioned. The condition number for the Eq. (2)-(4) is given in Table 2.

Table 2: The condition number of the surge, sway and yaw motion

	Surge	Sway	Yaw
Condition number	2.39E+23	9.49E+22	7.14E+21

The uncertainty of parameters is affected by noise and quantified by the error propagation matrix. The error propagation matrix or covariance matrix can be used to indicate how the random errors in y, as described by V_y, propagate to the optimal parameter $\hat{\theta}$. The error propagation matrix is given by

$$V_{\hat{\theta}} = \left[\frac{\partial \hat{\theta}}{\partial y} \right] V_y \left[\frac{\partial \hat{\theta}}{\partial y} \right]^T \qquad\qquad (29)$$

where the standard error of the parameters, $\sigma_{\hat{\theta}}$, can get by calculation of the square-root of the diagonal of the error propagation matrix. Then the absolute error can be calculated easily.

5.1 Parameter estimation using classical LS-SVM

In this phase, the classical LS-SVM will be employed to estimate the parameter of yaw motion. The linear kernel function is chosen, and the regularization factor, C, is chosen as 3500 considering the optimal parameter in Ref [41]. The obtained numerical model is used to reproduce the yaw moment of the validation set. The yaw model, as illustrated in Eq. 4, was chosen. The training process was carried out and the numerical prediction was compared with the experimental data, as presented in Fig. 6. The obtained model approximates the yaw moment in the training set successfully. However, the obtained hydrodynamic coefficients for yaw motion, as presented in Table 3, are obviously wrong. They do not have any physical meaning and drift from the true value largely. The validation process was carried out and the result was presented in Fig. 7. From the

figure, the obtained numerical yaw model failed to reproduce the yaw moment in the validation set. Obviously, the obtained numerical model overestimates the yaw moments. As discussed in the preceding section, the number of singular values of the kernel matrix equals to the length of the training set. so, they are 7000 singular values, and solutions are dominated by the smaller singular values seriously. The resulted parameters do not have any physical meaning and the generalization performance of the obtained model is poor. Therefore, in order to diminish the parameter drift, the optimal truncated LS-SVM proposed in the preceding section are used to estimate the hydrodynamic coefficients of nonlinear manoeuvring model.

Table 3. Values of the hydrodynamic coeffecent of yaw motion

Coef.	μ'_{26}	μ'_{66}	N'_0	N'_v
Value	-2.66E+06	-2.66E+06	-2.66E+06	-2.66E+06
Coef.	N'_r	$N'_{r\|v\|}$	$N'_{v\|r\|}$	$N'_{r\|r\|}$
Value	-4.83E+07	-4.83E+07	-4.83E+07	-4.83E+07
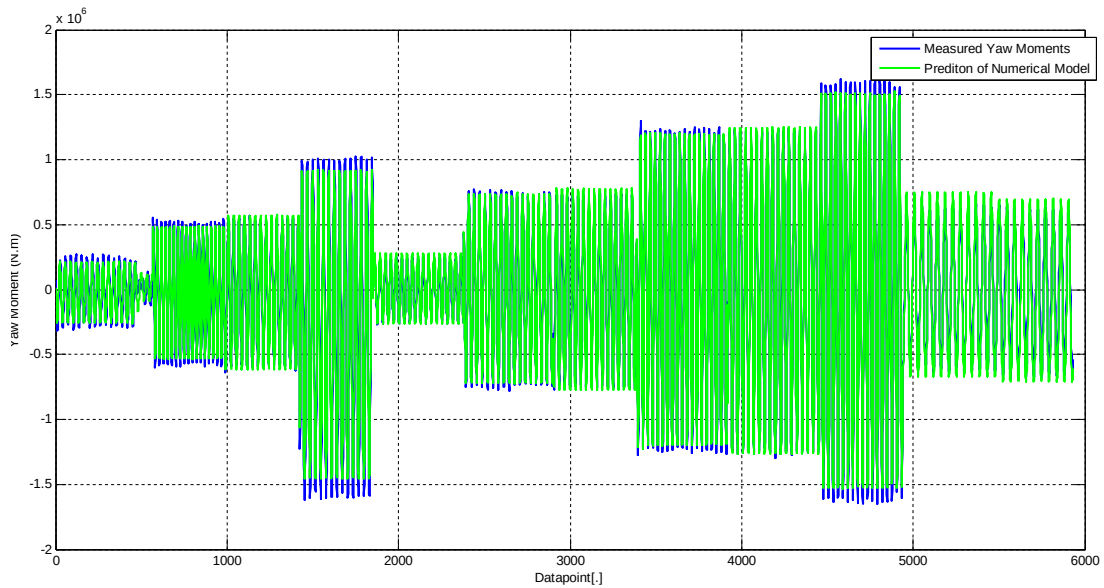
Fig. 6. The experimental data compares with the prediction of the numerical model obtained using classical LS-SVM during the training process.
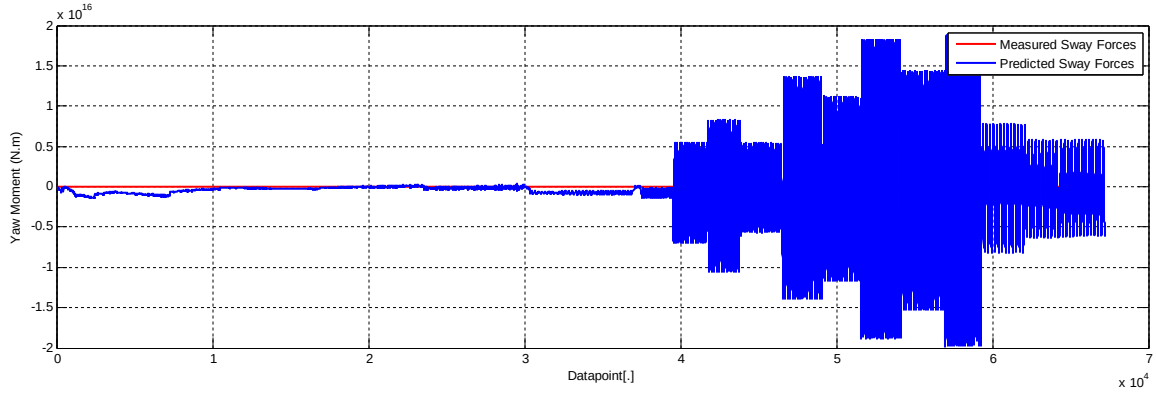
Fig. 7. The yaw moment reproduced using the obtained numerical model compared with the experimental results in the validation set.

5.2 Parameter estimation using optimal Truncated LS-SVM and validation

In this part, the optimal truncated LS-SVM was used to estimate the nondimensionalized hydrodynamic coefficients as defined in Eq. (2)-(4). As presented in the flowchart, the truncated LS-SVM can get a robust estimation by neglecting the smaller singular values, which usually contribute negligibly to the solutions and increase the parameter uncertainty. The optimal value, r, were estimated using *L-curve*. The results are presented in Table 4. Only a small number singular value was kept, for example, the optimal r equals to 437 for yaw motion. It means that around 5500 singular value can be neglected. For sway motion, the optimal r equals 1239, and r=4751 for surge motion.

Table 4: The optimal values of r using *L-Curve* for surge , sway , and yaw motion.

	Surge	Sway	Yaw
The optimal constant (r)	1751	1239	437

21

Table 5. The values of the parameters and its absolute error of the generic nonlinear manoeuvring model

Coef.	Values	Deviation (%)	Coef.	Values	Deviation (%)	Coef.	Values	Deviation (%)
μ'_{11}	7.33E-03	2.38	μ'_{22}	3.94E-02	0.55	μ'_{66}	1.12E-03	0.46
X'_0	-2.58E-04	3.91	Y'_0	-5.03E-04	6.71	μ'_{26}	-1.87E-03	1.45
X'_{vv}	-4.83E-03	5.17	Y'_v	-7.31E-02	0.77	N'_0	-3.50E-05	12.01
X'_{vr}	1.66E-02	2.85	Y'_r	2.30E-02	0.50	N'_v	-6.53E-03	0.70
X'_{rr}	-8.08E-04	9.25	$Y'_{v|v|}$	-3.37E-02	8.36	N'_r	-8.73E-03	0.44
			$Y'_{v|r|}$	-1.47E-02	9.78	$N'_{r|v|}$	-1.43E-02	1.08
						$N'_{v|r|}$	9.75E-03	1.92
						$N'_{r|r|}$	-1.87E-03	6.01

Fig. 8 presents the training results of surge (Fig. 8a), sway (Fig. 8b) and yaw motion (Fig. 8c). The resulted LS-SVM numerical model have a good agreement with the data in the training set. The obtained nondimensionalize hydrodynamic coefficients are presented in Table 5. The deviation is very smaller, which indicate that the parameter uncertainty is diminished successfully. The obtained parameters are very robust and less sensitive to noise in the measured data. The obtained values are near the true values.

Table 6. The values of the parameters and its absolute error of the Vectorial nonlinear manoeuvring model
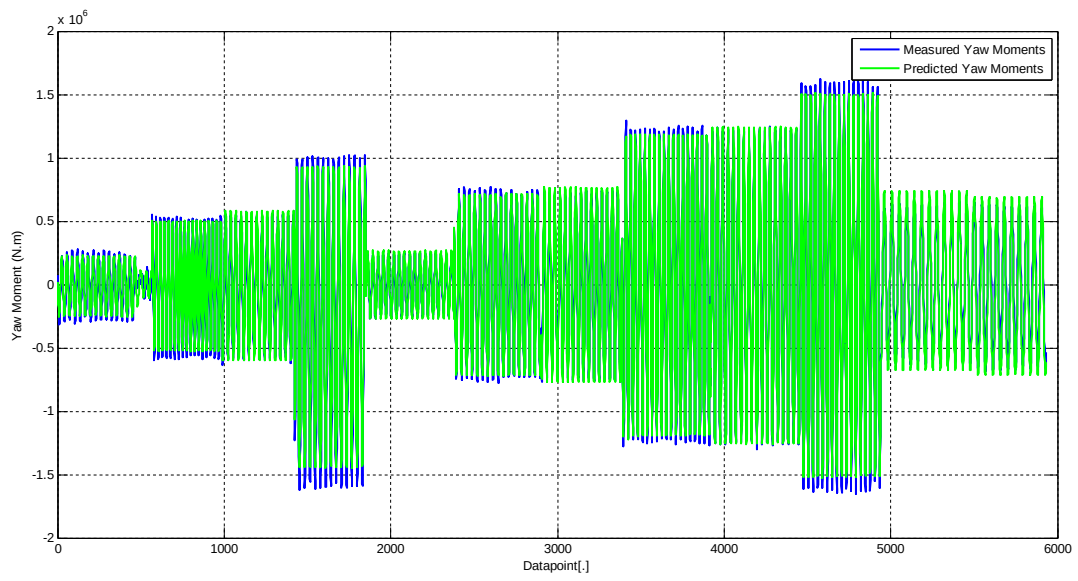
| Coef.	Value	Deviation (%)	Coef.	Value	Deviation (%)	Coef.	Value	Deviation (%)
$X'_{\dot{u}}$	-1.04E-02	0.61	$Y'_{\dot{v}}$	-3.82E-02	0.14	$N'_{\dot{r}}$	-1.20E-03	0.19
X'_{uuu}	-2.67E-04	1.29	$Y'_{\dot{r}}$	-2.66E-04	3.85	$N'_{\dot{v}}$	1.87E-03	0.65
X'_{uvv}	-9.29E-03	1.76	Y'_{uuv}	-6.16E-02	0.18	N'_{uur}	-8.41E-03	0.20
X'_{rvu}	5.84E-02	0.25	$Y'_{v|v|}$	-1.22E-01	0.28	$N'_{r|r|}$	-1.00E-03	2.50
X'_{urr}	-1.22E-03	2.33	Y'_{uur}	3.13E-02	0.09	N'_{uuv}	2.14E-02	0.10
			$Y'_{r|v|}$	1.12E-03	0.91	$N'_{v|r|}$	-1.69E-02	0.40
						$N'_{r|v|}$	1.11E-02	0.73
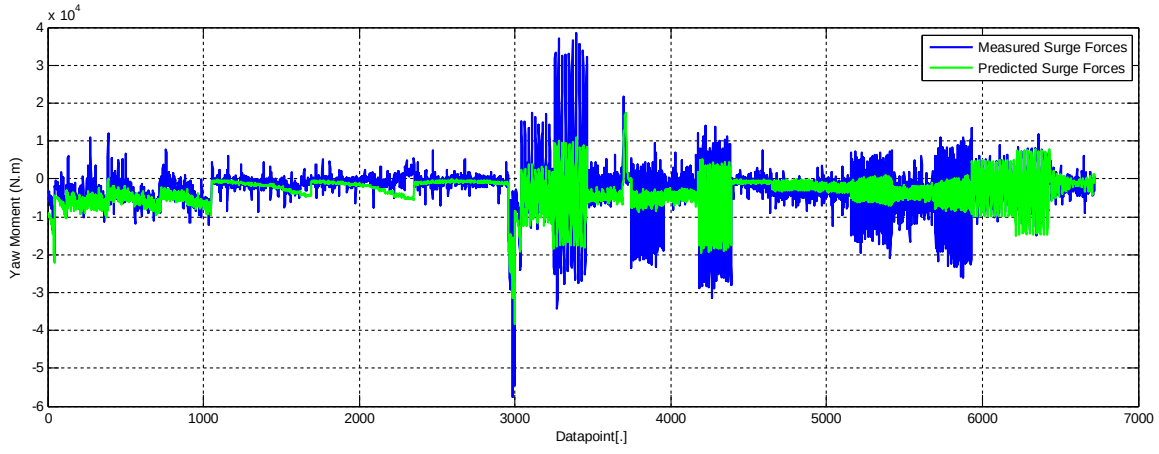
(a)
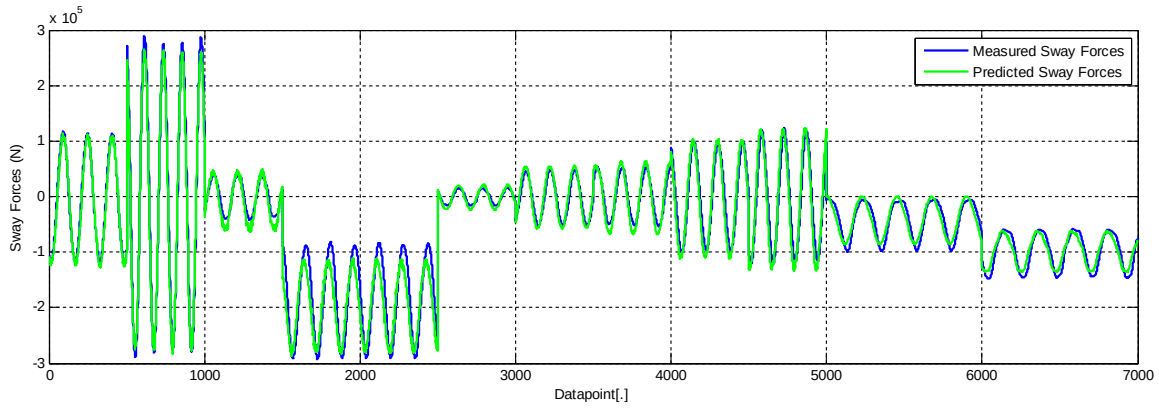
(b)

(c)

Fig. 8: The training process: the experiment data vs the prediction of the trained surge model (a), sway model (b), and yaw model(c).

Table 6 presents the obtained nondimensionalized hydrodynamic coefficients of vectorial nonlinear manoeuvring model defined in Eq.(13)-(15). The training process was using the optimal truncated LS-SVM. As observed from the previous discussion, these two manoeuvering model is different and proposed for a different purpose, meanwhile, the dimensional factors are also different. More details information about vectorial nonlinear manoeuvring model can be found in [61]. The vectorial model was proposed with emphasis placed on matrix properties like positiveness, symmetry and skew-symmetry. Those properties benefit the marine controller and observer design. However, the structure of these two models are different, but some parameters have the same values, as marked with the same colours in Table 6.and Table 7. For example, for add-mass and moment ($\mu_{11} \approx X'_{\dot{u}}; \mu_{22} \approx Y'_{\dot{v}}; \mu_{66} \approx N'_{\dot{r}}; \mu_{26} \approx N'_{\dot{v}}$); $X'_0 \approx X'_{uuu}$; $Y'_v \approx Y'_{uuv}$; $Y'_r = Y'_{uur}$; $N'_r \approx N'_{uur}$; $N'_{r|r|} \approx N'_{r|r|}$; $N'_{r|v|} \approx N'_{r|v|}$. So, the parameters of both models have the physical meaning, it describes the dynamics of ship motion. On the other hand, this also indicated the effectiveness of the proposed system identification method, optimal truncated LS-SVM.

Table 7: The R^2 values of the validation processes for the surge, sway and yaw motion

| R^2	Surge	Sway	Yaw
Generic model	0.6022	0.9723	0.9624
Vectorial model	0.5371	0.9811	0.9501

In order to test the generalization performance of the obtained numerical model, the data for validation, which was left completely untouched in the training, was used to validate the obtained numerical models. The results are presented in Fig. 9. Fig. 9 shows the prediction of forces and moments using the generic model compared with training data. In order to show the details of the figure, the partial enlargement of the figures are also given in the figure. From this figure, the curves fit well with each other, especially for sway force and yaw moments. R^2 values of the obtained generic models are 0.60, 0.97 and 0.96, respectively. A similar process are also carried out using the vectorial model, as presented in Fig. 10. The R^2 values are used to measure the goodness-of-fit, as presented in Table 7. Both nonlinear manoeuvring models have a very good generalization performance.
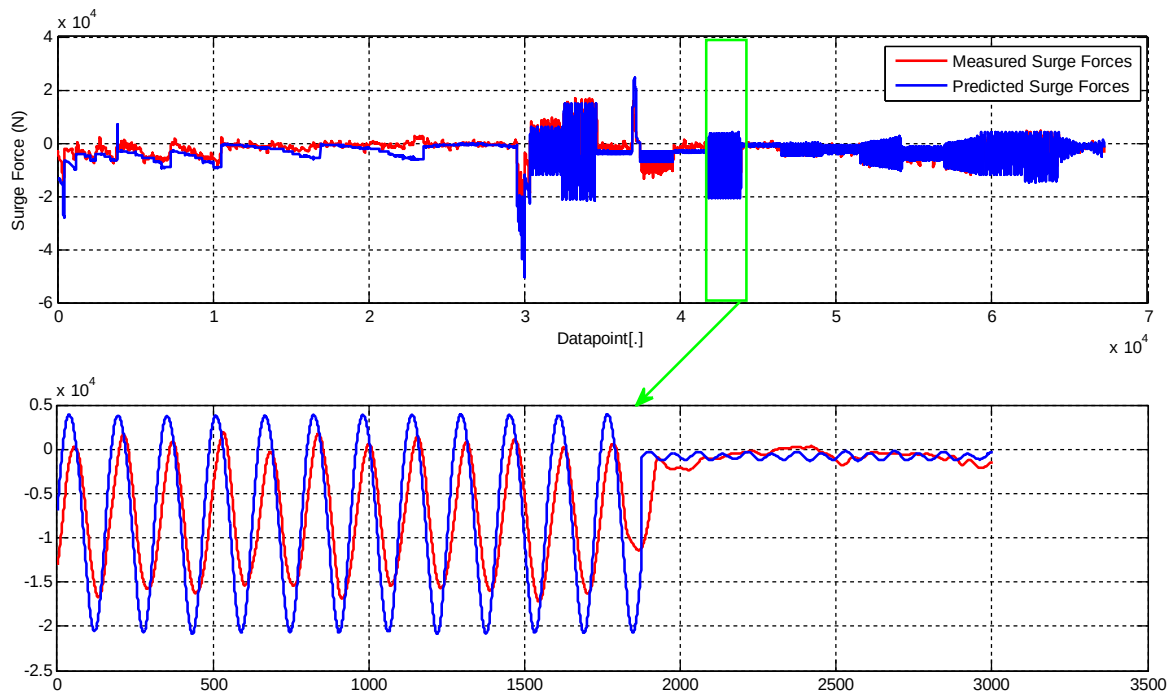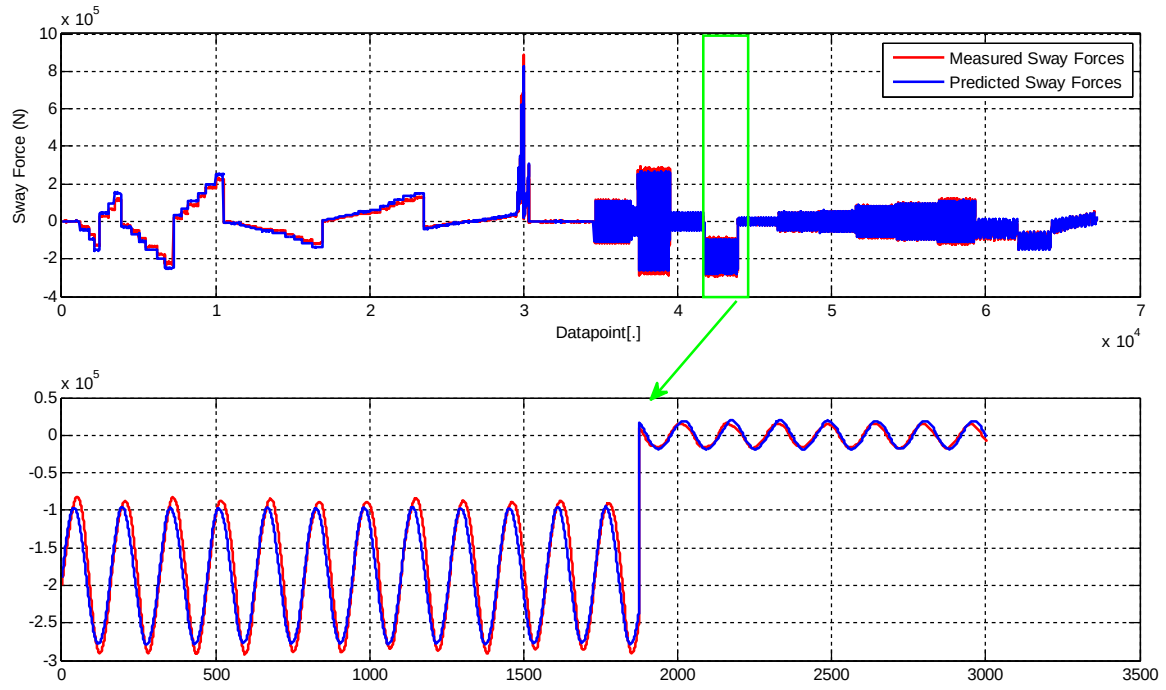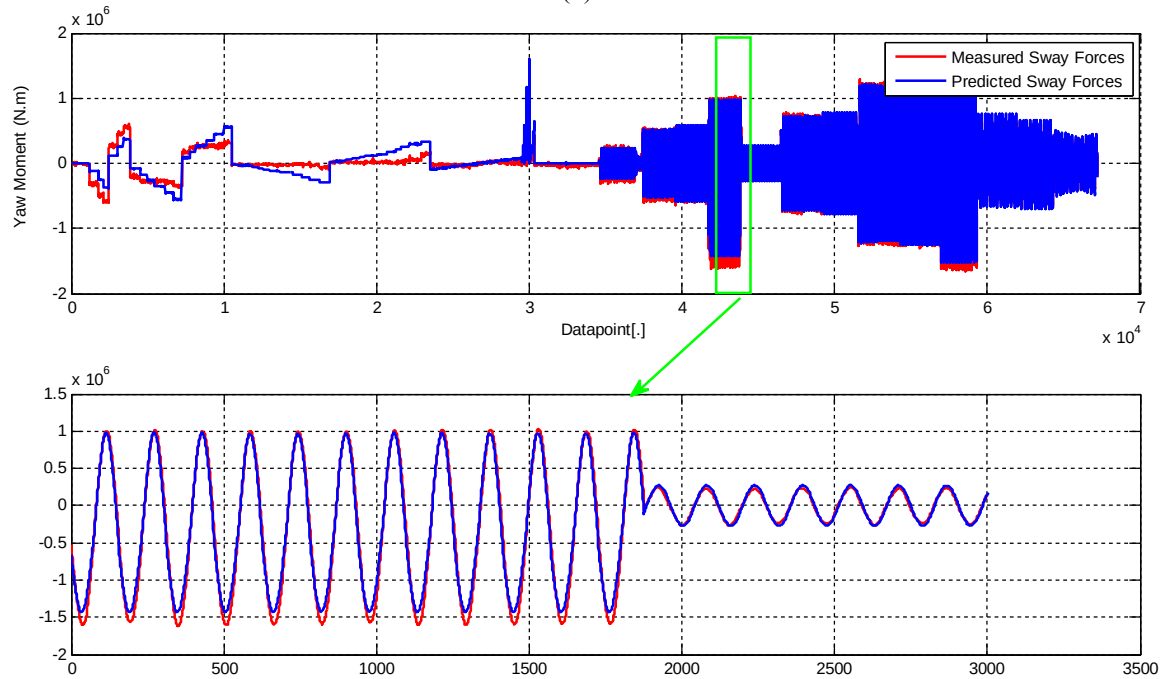
(a)

(b)

25
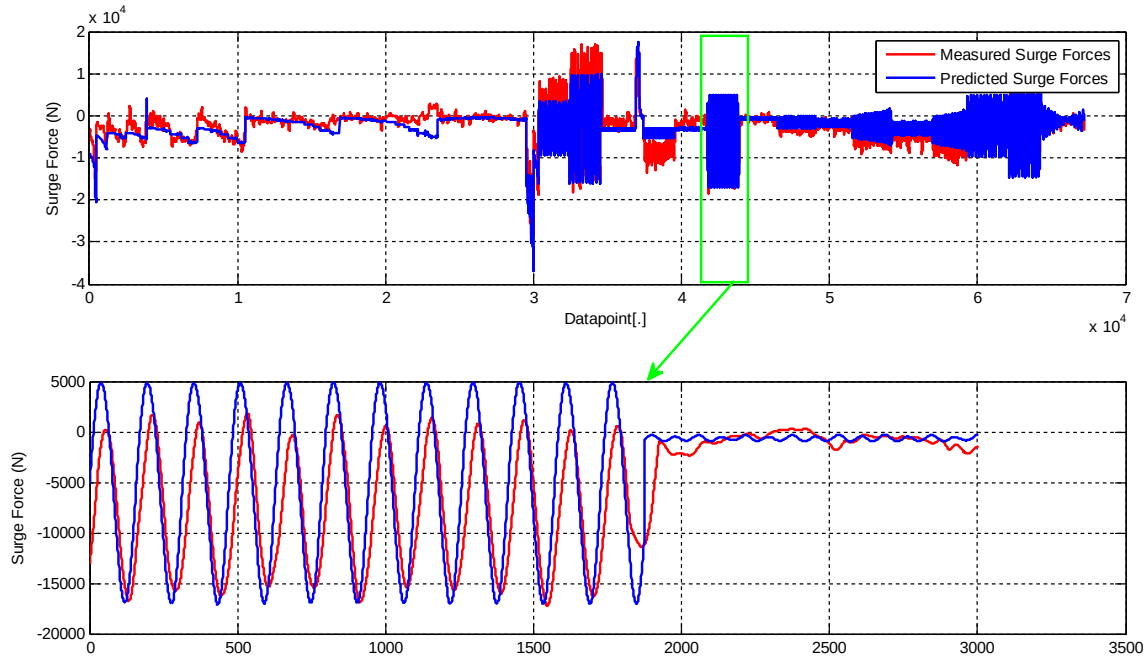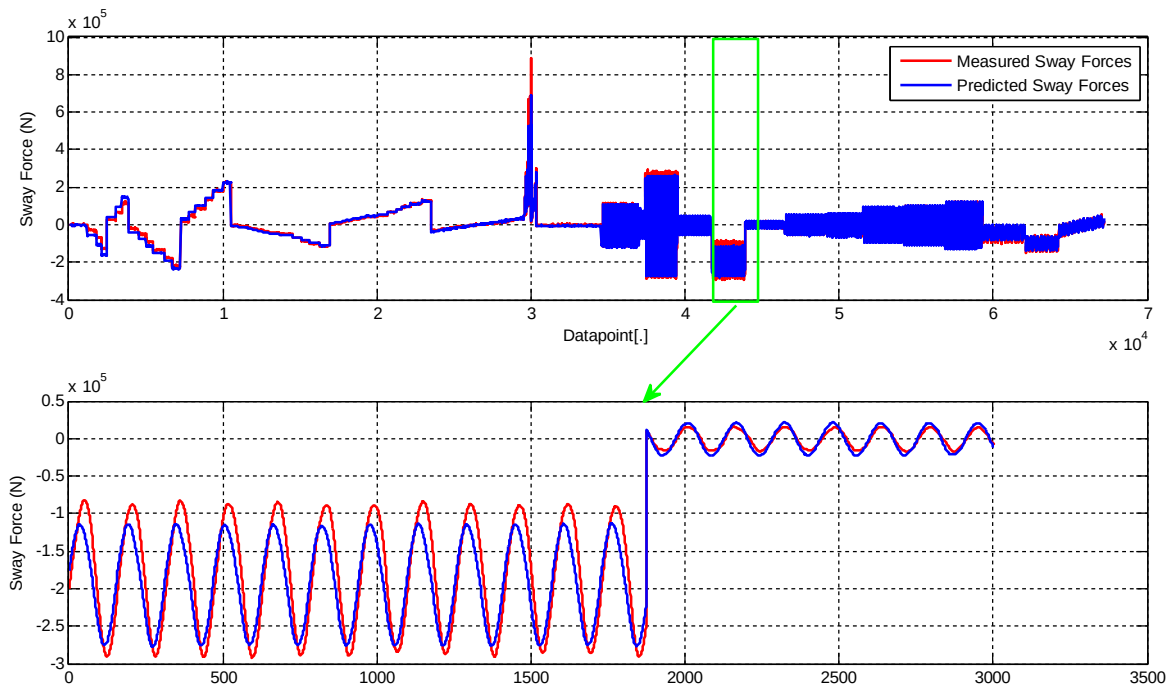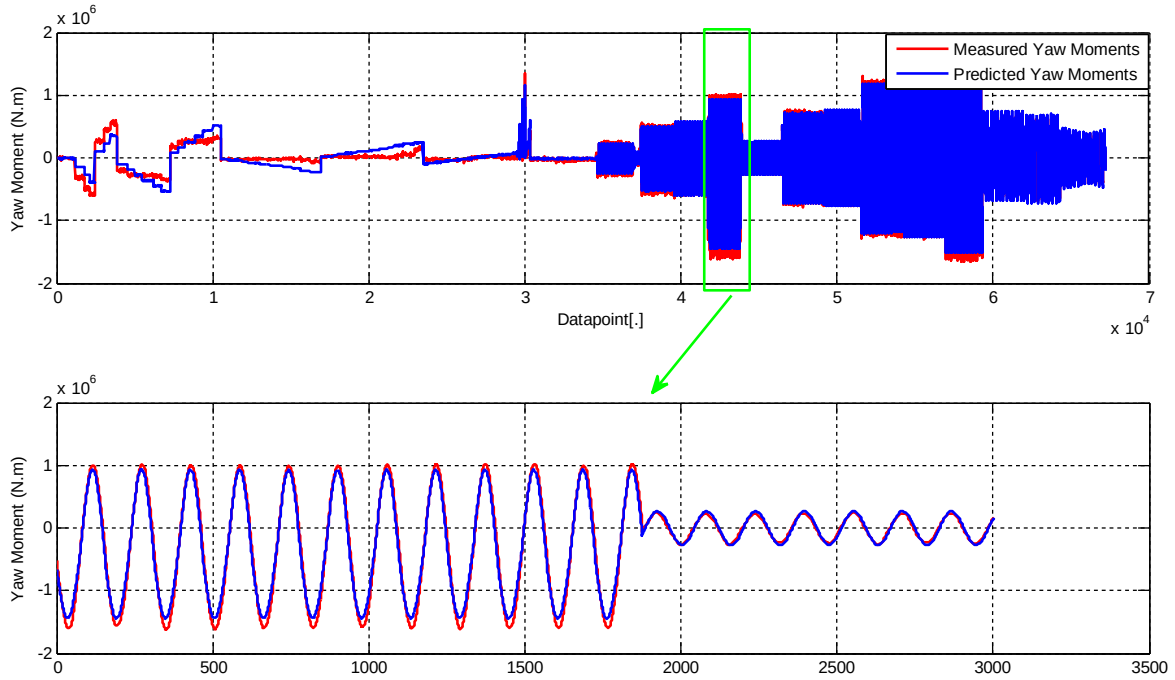
(c)

Fig. 9. The validation of the generic models: the experimenal data vs the prediciton (a: surge model; b: sway model; c: yaw model).

(a)

(b)

(c)

Fig. 10. The validation of the vectorial models: the experimenal data vs the prediciton (a: surge model; b: sway model; c: yaw model).

27

CONCLUSIONS

In this paper, an optimal truncated least square support vector machine was proposed to estimate the nondimensionalized coefficients of nonlinear manoeuvring models based on the captive model tests. Firstly, in order to describe the dynamics of the marine surface ship, two classical nonlinear manoeuvring models in 3-DOFs (surge, sway and yaw) were introduced. The generic nonlinear manoeuvring model is widely used to describe the manoeuvres of ships. The vectorial model is derived using Lagrange's method and widely employed for marine control application due to the matrix properties, such as positive, symmetry and skew-symmetry *et. al.* the hydrodynamic coefficients have been converted to the dimensionless ones using the prime system of SNAME (1950). PMM tests, such as pure surge, pure drift, pure sway, pure yaw and mixed sway and yaw, were carried out in SINTEF Ocean's multi-purpose towing tank using the scaled ship model. Optimal Truncated LS-SVM was proposed in order to get a robust parameter estimation. It can avoid the costly matrix inversion operation in classical LS-SVM by using the singular values decomposition. Meanwhile, the smaller singular values are neglected considering their contribution to the solutions is negligible and, sometimes increase the uncertainty in the solutions. The parameter with a large uncertainty indicated the parameter is sensitive to the noise in the data and have a poor generalization performance. As discussed in the paper, when the training set is large, the obtained parameters using classical LS-SVM are meaningless and usually drift from the true values. The parameter uncertainty for both nonlinear manoeuvring models was discussed. Although these two models were proposed for the different applications, some estimated coefficients have similar value, especially the linear terms, which indicates the robustness of the optimal truncated LS-SVM. The generalization performance of the resulted numerical models was further tested against the validation set, which was completely left untouched in the training. The R2 goodness of fit criterion was used to demonstrate the accuracy of the obtained models. The results show that both nonlinear manoeuvring models have a very good generalization performance.

REFERENCES

[1] A.J. Sørensen, A survey of dynamic positioning control systems, Annu. Rev. Control. 35 (2011) 123–136. doi:10.1016/J.ARCONTROL.2011.03.008.

[2] D. de A. Fernandes, A.J. Sørensen, K.Y. Pettersen, D.C. Donha, Output feedback motion control system for observation class ROVs based on a high-gain state observer: Theoretical and experimental results, Control Eng. Pract. 39 (2015) 90–102. doi:10.1016/J.CONENGPRAC.2014.12.005.

[3] P. Ridao, M. Carreras, D. Ribas, P.J. Sanz, G. Oliver, Intervention AUVs: The next challenge, Annu. Rev. Control. 40 (2015) 227–241. doi:10.1016/J.ARCONTROL.2015.09.015.

[4] J.M. Varela, C. Guedes Soares, Software architecture of an interface for three-dimensional collision handling in maritime Virtual Environments, Simulation. 91 (2015) 735–749. doi:10.1177/0037549715598008.

[5] J.M. Varela, C. Guedes Soares, Interactive 3D desktop ship simulator for testing and training offloading manoeuvres, Appl. Ocean Res. 51 (2015) 367–380. doi:10.1016/J.APOR.2015.01.013.

[6] M.A. Abkowitz, Measurement of hydrodynamic characteristics from ship maneuvering trials by system identification, SNAME Trans. 88 (1980) 283–318. https://trid.trb.org/view/157366 (accessed April 7, 2018).

[7] W. Hwang, Application of System Identification to Ship Maneuvering, Massachusetts Institute of Technology, 1980. https://dspace.mit.edu/bitstream/handle/1721.1/15820/08049757-MIT.pdf?sequence=2 (accessed April 24, 2018).

[8] H. Xu, M.A. Hinostroza, C. Guedes Soares, Estimation of Hydrodynamic Coefficients of a Nonlinear

Manoeuvring Mathematical Model With Free-Running Ship Model Tests, Int. J. Marit. Eng. Vol 160 (2018) A-213-A-226. doi:10.3940/rina.ijme.a3.2018.448.

[9]   Y. Yoshimura, Mathematical model for manoeuvring ship motion (MMG Model), in: Work. Math. Model. Oper. Involv. Ship-Sh. Interact., Kansai Zōsen Kyōkai Kyōkai, 2005: pp. 1–6. https://trid.trb.org/view/391815 (accessed April 29, 2018).

[10]   K. Nomoto, K. Taguchi, K. Honda, S. Hirano, On the Steering Qualities of Ships, J. Zosen Kiokai. 1956 (1956) 75–82. doi:10.2534/jjasnaoe1952.1956.99_75.

[11]   T.I. Fossen, Handbook of Marine Craft Hydrodynamics and Motion Control, John Wiley & Sons, Ltd, Chichester, UK, 2011. doi:10.1002/9781119994138.

[12]   S. Sutulo, C. Guedes Soares, Development of a core mathematical model for arbitrary manoeuvres of a shuttle tanker, Appl. Ocean Res. 51 (2015) 293–308. doi:10.1016/j.apor.2015.01.008.

[13]   S. Sutulo, C. Guedes Soares, Mathematical models for simulation of manoeuvring performance of ships, in: C. Guedes Soares, Y. Garbatov, N. Fonseca, A.P. Teixeira (Eds.), Marit. Eng. Technol., Taylor & Francis Group, London, 2011: pp. 661–698. doi:10.13140/2.1.3538.7209.

[14]   ITTC, Final Report and Recommendations to the 24th ITTC, in: 24th Int. Towing Tank Conf., 2005: pp. 369–408. https://www.google.pt/ (accessed July 24, 2018).

[15]   S. Sutulo, C. Guedes Soares, Development of a Multifactor Regression Model of Ship Maneuvering Forces Based on Optimized Captive-Model Tests, J. Sh. Res. 50 (2006) 311–333. https://www.ingentaconnect.com/content/sname/jsr/2006/00000050/00000004/art00002 (accessed July 1, 2018).

[16]   L. Ljung, System identification : theory for the user, Prentice Hall PTR, 1999.

[17]   B. Golding, A. Ross, T.I. Fossen, Identification of nonlinear viscous damping for marine vessels, in: 14 Th IFAC Symp. Syst. Identif., Newcastle , Australia , 2006, 2006: pp. 332–337. doi:https://doi.org/10.3182/20060329-3-AU-2901.00048.

[18]   S. Sutulo, C. Guedes Soares, An algorithm for offline identification of ship manoeuvring mathematical models from free-running tests, Ocean Eng. 79 (2014) 10–25. doi:10.1016/j.oceaneng.2014.01.007.

[19]   W.L. Luo, Z.J. Zou, Parametric Identification of Ship Maneuvering Models by Using Support Vector

Machines, J. Sh. Res. 53 (2009) 19–30.

[20] W. Luo, L. Moreira, C. Guedes Soares, Manoeuvring simulation of catamaran by using implicit models based on support vector machines, Ocean Eng. 82 (2014) 150–159. doi:10.1016/j.oceaneng.2014.03.008.

[21] K.J. Åström, C.G. Källström, Identification of ship steering dynamics, Automatica. 12 (1976) 9–22. doi:10.1016/0005-1098(76)90064-9.

[22] A. Ross, O. Selvik, V. Hassani, E. Ringen, D. Fathi, Identification of Nonlinear Manoeuvring Models for Marine Vessels using Planar Motion Mechanism Tests, in: ASME 2015 34th Int. Conf. Ocean. Offshore Arct. Eng., ASME, Newfoundland, Canada, 2015: p. V007T06A014. doi:10.1115/OMAE201541789.

[23] P.W.J. van de Ven, T.A. Johansen, A.J. Sørensen, C. Flanagan, D. Toal, Neural network augmented identification of underwater vehicle models, Control Eng. Pract. 15 (2007) 715–725. doi:10.1016/J.CONENGPRAC.2005.11.004.

[24] V. Hassani, D. Fathi, A. Ross, F. Sprenger, Ø. Selvik, T.E.T.E. Berg, D. Fathi, F. Sprenger, T.E.T.E. Berg, Time domain simulation model for research vessel Gunnerus, in: ASME 2015 34th Int. Conf. Ocean. Offshore Arct. Eng., ASME, Newfoundland, Canada, 2015: p. V007T06A013. doi:10.1115/OMAE201541786.

[25] G.H. Golub, C. Reinsch, Singular value decomposition and least squares solutions, Numer. Math. 14 (1970) 403–420. doi:10.1007/BF02163027.

[26] T.F. Chan, P.C. Hansen, Computing Truncated Singular Value Decomposition Least Squares Solutions by Rank Revealing QR-Factorizations, SIAM J. Sci. Stat. Comput. 11 (1990) 519–530. doi:10.1137/0911029.

[27] P. Hansen, Rank-deficient and discrete ill-posed problems: numerical aspects of linear inversion, Soc. Ind. Appl. Math. (1998) 175–208. doi:http://dx.doi.org/10.1137/1.9780898719697.

[28] J.B. Bell, A.N. Tikhonov, V.Y. Arsenin, Solutions of Ill-Posed Problems., Math. Comput. 32 (1978) 1320–1322. doi:10.2307/2006360.

[29] T. Söderström, Comparing some classes of bias-compensating least squares methods, Automatica. 49 (2013) 840–845. doi:10.1016/j.automatica.2013.01.003.

[30]   G.H. Golub, P.C. Hansen, D.P. O'Leary, Tikhonov Regularization and Total Least Squares, SIAM J. Matrix Anal. Appl. 21 (1999) 185–194. doi:10.1137/S0895479897326432.

[31]   P.C. Hansen, D.P. O'Leary, The Use of the L-Curve in the Regularization of Discrete Ill-Posed Problems, SIAM J. Sci. Comput. 14 (1993) 1487–1503. doi:10.1137/0914086.

[32]   D. Ma, W. Tan, Z. Zhang, J. Hu, Parameter identification for continuous point emission source based on Tikhonov regularization method coupled with particle swarm optimization algorithm, J. Hazard. Mater. 325 (2017) 239–250. doi:10.1016/J.JHAZMAT.2016.11.071.

[33]   V. Hassani, A.J. Sørensen, A.M. Pascoal, Adaptive wave filtering for dynamic positioning of marine vessels using maximum likelihood identification: Theory and experiments, in: IFAC Proc. Vol., 2013: pp. 203–208. doi:10.3182/20130918-4-JP-3022.00041.

[34]   L.P. Perera, P. Oliveira, C. Guedes Soares, System Identification of Nonlinear Vessel Steering, J. Offshore Mech. Arct. Eng. 137 (2015) 031302. doi:10.1115/1.4029826.

[35]   L.P. Perera, P. Oliveira, C. Guedes Soares, System identification of vessel steering with unstructured uncertainties by persistent excitation maneuvers, IEEE J. Ocean. Eng. 41 (2016) 515–528. doi:10.1109/JOE.2015.2460871.

[36]   J.A.K. Suykens, J. Vandewalle, Least Squares Support Vector Machine Classifiers, Neural Process. Lett. 9 (1999) 293–300. doi:10.1023/A:1018628609742.

[37]   V.N. Vapnik, The Nature of Statistical Learning Theory, Springer. 8 (1995) 187. doi:10.1109/TNN.1997.641482.

[38]   H. Xu, C. Guedes Soares, Vector field path following for surface marine vessel and parameter identification based on LS-SVM, Ocean Eng. 113 (2016) 151–161. doi:10.1016/j.oceaneng.2015.12.037.

[39]   H.T. Xu, C. Guedes Soares, Waypoint-following for a marine surface ship model based on vector field guidance law, in: C. Guedes Soares, T.A. Santos (Eds.), Marit. Technol. Eng. 3, Taylor & Francis Group, London, UK, 2016: pp. 409–418.

[40]   H.T. Xu, M.A. Hinostroza, C. Guedes Soares, A hybrid controller design for ship autopilot based on free-running model test, in: C. Guedes Soares, A.P. Teixeir (Eds.), Marit. Transp. Harvest. Sea Resour., Taylor & Francis Group, London, UK, 2017: pp. 1051–1059.

[41] W. Luo, C. Guedes Soares, Z. Zou, Parameter Identification of Ship Maneuvering Model Based on Support Vector Machines and Particle Swarm Optimization, J. Offshore Mech. Arct. Eng. 138 (2016) 031101. doi:10.1115/1.4032892.

[42] X.-R. Hou, Z.-J. Zou, Parameter identification of nonlinear roll motion equation for floating structures in irregular waves, Appl. Ocean Res. 55 (2016) 66–75. doi:10.1016/J.APOR.2015.11.007.

[43] M. Zhu, A. Hahn, Y.-Q. Wen, A. Bolles, Identification-based simplified model of large container ships using support vector machines and artificial bee colony algorithm, Appl. Ocean Res. 68 (2017) 249–261. doi:10.1016/J.APOR.2017.09.006.

[44] W. Luo, X. Li, Measures to diminish the parameter drift in the modeling of ship manoeuvring using system identification, Appl. Ocean Res. 67 (2017) 9–20. doi:10.1016/j.apor.2017.06.008.

[45] H.T. Xu, V. Hassani, C. Guedes Soares, Parameters Estimation of Nonlinear Manoeuvring Model for Marine Surface Ship Based on PMM Tests, in: ASME 2018 37th Int. Conf. Ocean. Offshore Arct. Eng., ASME, Madrid, spain, 2018: p. V11BT12A010. doi:10.1115/OMAE2018-78235.

[46] T. Wei, S. Zhongke, L. Hongchao, Denoising of impulse response using LS-SVM and SVD for aircraft flight flutter test, in: Syst. Control Aerosp. Astronaut. 2006. ISSCAA 2006. 1st Int. Symp., IEEE, 2006: pp. 684. – 688. doi:10.1109/ISSCAA.2006.1627426.

[47] P.-P. Zheng, J. Feng, Z. Li, M. Zhou, A novel SVD and LS-SVM combination algorithm for blind watermarking, Neurocomputing. 142 (2014) 520–528. doi:10.1016/J.NEUCOM.2014.04.005.

[48] O.M. Faltinsen, Hydrodynamics of High-Speed Marine Vehicles, Cambridge University Press, Cambridge, 2006. doi:10.1017/CBO9780511546068.

[49] SNAME, Nomenclature for treating the motion of a submerged body through a fluid, Society of Naval Architects and Marine Engineers, New York, 1950. http://www.worldcat.org/title/nomenclature-for-treating-the-motion-of-a-submerged-body-through-a-fluid-report-of-the-american-towing-tank-conference/oclc/21074219 (accessed April 24, 2018).

[50] W. Caharija, K.Y. Pettersen, M. Bibuli, P. Calado, E. Zereik, J. Braga, J.T. Gravdahl, A.J. Sorensen, M. Milovanovic, G. Bruzzone, Integral Line-of-Sight Guidance and Control of Underactuated Marine Vehicles: Theory, Simulations, and Experiments, IEEE Trans. Control Syst. Technol. 24 (2016) 1623–1642. doi:10.1109/TCST.2015.2504838.

[51] T.I. Fossen, A.M. Lekkas, Direct and indirect adaptive integral line-of-sight path-following controllers for marine craft exposed to ocean currents, Int. J. Adapt. Control Signal Process. 31 (2015) 445–463. doi:10.1002/acs.2550.

[52] S.P. Berge, T.I. Fossen, On the Properties of the Nonlinear Ship Equations of Motion, Math. Comput. Model. Dyn. Syst. 6 (2000) 365–381. doi:10.1076/mcmd.6.4.365.3660.

[53] A.J. Sørensen, Marine Control Systems Propulsion and Motion Control of Ships and Ocean Structures Lecture Notes, 2012. http://citeseerx.ist.psu.edu/viewdoc/summary?doi=10.1.1.296.6035 (accessed May 23, 2018).

[54] S. Inoue, M. Hirano, K. Kijima, J. Takashina, A practical calculation method of ship maneuvering motion, Int. Shipbuild. Prog. 28 (1981) 207–222. doi:10.3233/ISP-1981-2832502.

[55] J.A.K. Suykens, T. Van Gestel, J. De Brabanter, B. De Moor, J. Vandewalle, Least Squares Support Vector Machines, 2002. doi:10.1142/9789812776655.

[56] V.N. Vapnik, Statistical Learning Theory, 1998. doi:10.2307/1271368.

[57] L. Chen, S. Zhou, Sparse algorithm for robust LSSVM in primal space, Neurocomputing. 275 (2018) 2880–2891. doi:10.1016/j.neucom.2017.10.011.

[58] P.C. Hansen, P.R. Johnston, The L-Curve and its Use in the Numerical Treatment of Inverse Problems, in: Comput. Inverse Probl. Electrocardiogr., 2001: pp. 119–142. file://g/Publications/PDFs/hansen2001_Lcurve.pdf.

[59] SimVal, Sea Trials and Model Tests for Validation of Shiphandling Simulation Models (SimVal), (n.d.). https://www.sintef.no/projectweb/simval/ (accessed April 26, 2018).

[60] ITTC, Manoeuvrability Captive Model Test Procedure, in: 23rd Int. Towing Tank Conf., 2002. http://www.simman2008.dk/PDF/7.5-02-06-02 (captive model tests).pdf (accessed April 26, 2018).

[61] H. Xu, V. Hassani, C. Guedes Soares, Uncertainty analysis of the hydrodynamic coefficients estimation of a nonlinear manoeuvring model based on planar motion mechanism tests, Ocean Eng. 173 (2019) 450–459. doi:10.1016/j.oceaneng.2018.12.075.